DOI: 10.3901/CJME.2015.1120.137, available online at www.springerlink.com; www.cjmenet.com

Rapid Optimization of Tension Distribution for Cable-Driven Parallel Manipulators with Redundant Cables

OUYANG Bo and SHANG Weiwei*

Department of Automation, University of Science and Technology of China, Hefei 230027, China

Received April 10, 2015; revised November 12, 2015; accepted November 20, 2015

Abstract: The solution of tension distributions is infinite for cable-driven parallel manipulators(CDPMs) with redundant cables. A rapid optimization method for determining the optimal tension distribution is presented. The new optimization method is primarily based on the geometry properties of a polyhedron and convex analysis. The computational efficiency of the optimization method is improved by the designed projection algorithm, and a fast algorithm is proposed to determine which two of the lines are intersected at the optimal point. Moreover, a method for avoiding the operating point on the lower tension limit is developed. Simulation experiments are implemented on a six degree-of-freedom(6-DOF) CDPM with eight cables, and the results indicate that the new method is one order of magnitude faster than the standard simplex method. The optimal distribution of tension distribution is thus rapidly established on real-time by the proposed method.

Keywords: cable-driven parallel manipulator, tension distribution, redundant cable, linear programming

1 Introduction

Cable-driven parallel manipulators(CDPMs) are a special type of parallel mechanism in which a moving platform is driven by cables instead of rigid links. This particular structure provides CDPMs several advantages, such as larger workspaces, a higher payload-to-weight ratio and lower manufacturing costs, versus a parallel manipulator with rigid links. CDPMs are therefore more suitable for high-load and high-acceleration applications. A wide variety of CDPMs have been developed[1–3] and applied in engineering equipment, such as an aircraft wind tunnel test[4], a large radio telescope[5], a human movement training system[6–7], and a seven degree-of-freedom(7-DOF) cable-driven robotic arm[8].

However, cables are flexible and elastic, and they will sag under the effect of their own weights. Moreover, the mass of cables will change when the end effector moves[9]. These characteristics of cables bring huge challenge to the motion control of CDPMs[10]. The first key problem to the motion control is that cables of a CDPM can only work in tension, i.e., cables are unable to push the moving platform. To overcome this limitation, a wrench-closure workspace has been proposed to generate only positive tension[11–13]. In general, the number of cables m must be larger than the DOF n to satisfy the wrench-closure condition. However, the range of tensions for a wrench-closure workspace is often assumed to be unlimited, even though this is impractical. Thus, a wrench feasible workspace should be defined so that the tension in each cable remains within a prescribed range[14–16]. However, for a completely($m=n+1$) or redundantly restrained CDPM($m>n+1$), there exist an infinite number of tension distributions. Therefore, the optimal tension distribution should be determined with respect to some useful objective function.

For a completely restrained CDPM, the null space of a structure matrix is one dimensional, and the solution set is a line segment. To solve this single-variable optimization problem, FANG, et al[17], proposed an efficient algorithm for the completely restrained CDPM. In addition, LI, et al[18], applied the Levenberg-Marquardt method for a five hundred meter aperture spherical telescope(FAST) in which the gravity was considered as a virtual cable and the cable catenary was taken into account. For a 2-DOF CDPM with four cables, a hexagon is the most complex case of the solution set, and a fast optimization method is proposed by using the geometry property[19]. However, with the increasing number of DOFs and cables, the solution set becomes more and more complex, and the computational time increases rapidly.

If the sum of all tensions is used as the objective function, then the optimization of tension distribution becomes a linear programming problem. However, MIKELSONS, et al[20], indicated that the tension distribution obtained by

* Corresponding author. E-mail: wwshang@ustc.edu.cn
Supported by National Natural Science Foundation of China(Grant No. 51275500), Research Project of State Key Laboratory of Mechanical System and Vibration(Grant No. MSV201502), USTC-COOGOO Robotics Research Center(Grant No. 2015), and Youth Innovation Promotion Association of Chinese Academy of Sciences(Grant No. 2012321)

linear programming was discontinuous and that high-frequency oscillations may result from changes in tension. As the number of cables increase, the method proposed by MIKELSONS et al is too complex to satisfy the real-time requirement. BOGSTROM, et al[21], introduced a slack variable in the inequality constraint to obtain the optimal tension distribution, but they did not prove the continuity of the tension distribution. HASSAN, et al[22], defined the two-norm of the tension distribution as the objective function and applied Dykstra's method to compute the optimal tension distribution. However, their optimization method requires a large number of iterations to converge, and the computational efficiency still needs to be improved.

Although the simplex method is well known for solving linear programming, it needs a feasible starting point to solve the optimization problem. Unfortunately, finding these starting points is generally nontrivial. In this paper, we present a projection algorithm designed for obtaining a feasible starting point fast by using the geometry property of a polyhedron. Interestingly, a starting point is also a candidate solution for avoiding the operating point on the lower tension limit. The efficiency of our projection algorithm comes from a reduced number of extreme points that need to be checked to obtain an optimal point. The key to this reduction is a rapid algorithm that finds the two lines intersecting at the optimal point based on convex analysis. With our projection algorithm, a new and efficient optimization method can be obtained for CDPMs with redundant cables. Simulation experiments implemented on a 6-DOF CDPM with eight cables show that this new optimization method is considerably faster than the simplex method.

The rest of this paper is organized as follows. In section 2, the static model of an n-DOF CDPM is established. In section 3, the cable tension solution is given for CDPMs with redundant cables. In section 4, a new rapid optimization method is proposed, and detailed design procedures are described. In section 5, simulation experiments are implemented on a 6-DOF CDPM with eight cables. Finally, concluding remarks are presented in section 6.

2 Static CDPM Model

A CDPM is a closed-loop mechanism including multiple kinematic chains in which a moving platform and static platform are connected by cables. The structural diagram of an n-DOF CDPM with m cables is shown in Fig. 1 in which coordinate frame O is the base frame and coordinate frame P is the local frame fixed on the moving platform. Here, the gravity of the cables is neglected, and each cable is considered a straight line in static equilibrium.

Based on the force equilibrium of the moving platform, the static equation of the system is given by

$$\begin{cases} \sum_{i=1}^{m} \boldsymbol{t}_i + \boldsymbol{F} = 0, \\ \sum_{i=1}^{m} \boldsymbol{r}_i \times \boldsymbol{t}_i + \boldsymbol{M} = 0, \end{cases} \tag{1}$$

where $\boldsymbol{t}_i$—Cable tension,

$\boldsymbol{r}_i = \boldsymbol{PP}_i$,

$\boldsymbol{F}$—External force applied on the move platform,

$\boldsymbol{M}$—Moment applied on the moving platform.

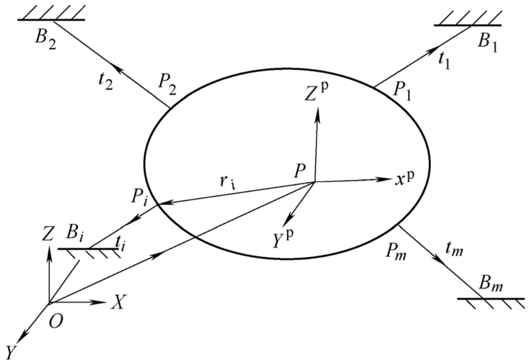

Fig. 1. Structural diagram of an n-DOF CDPM

Let $\boldsymbol{u}_i$ ($\boldsymbol{P}_i\boldsymbol{B}_i$) represent the unit vector of $\boldsymbol{t}_i$, and t_i represents the magnitude of the cable tension. Then, the matrix form of Eq. (1) can be written as

$$\boldsymbol{A} \bullet \boldsymbol{T} = \boldsymbol{W}, \tag{2}$$

where $\boldsymbol{T} = (t_1 \quad t_2 \quad \cdots \quad t_m)^{\mathrm{T}} \in \mathbf{R}^m$,

$$\boldsymbol{W} = -\begin{pmatrix} \boldsymbol{F} \\ \boldsymbol{M} \end{pmatrix} \in \mathbf{R}^n,$$

$$\boldsymbol{A} = \begin{pmatrix} \boldsymbol{u}_1 & \boldsymbol{u}_2 & \cdots & \boldsymbol{u}_m \\ \boldsymbol{r}_1 \times \boldsymbol{u}_1 & \boldsymbol{r}_2 \times \boldsymbol{u}_2 & \cdots & \boldsymbol{r}_m \times \boldsymbol{u}_m \end{pmatrix}.$$

Here let superscript p denote the vectors in coordinate frame P, and $\boldsymbol{R}$ represents the orientation of coordinate frame P with respect to the coordinate frame O, and $\boldsymbol{R}$ is defined by

$$\boldsymbol{R} = \begin{pmatrix} \mathrm{c}\alpha\,\mathrm{c}\beta & -\mathrm{s}\alpha\,\mathrm{c}\gamma + \mathrm{c}\alpha\,\mathrm{s}\beta\,\mathrm{s}\gamma & \mathrm{s}\alpha\,\mathrm{s}\gamma + \mathrm{c}\alpha\,\mathrm{s}\beta\,\mathrm{c}\gamma \\ \mathrm{s}\alpha\,\mathrm{c}\beta & \mathrm{c}\alpha\,\mathrm{c}\gamma + \mathrm{s}\alpha\,\mathrm{s}\beta\,\mathrm{s}\gamma & -\mathrm{c}\alpha\,\mathrm{s}\gamma + \mathrm{s}\alpha \bullet \mathrm{s}\beta\,\mathrm{c}\gamma \\ -\mathrm{s}\beta & \mathrm{c}\beta\,\mathrm{s}\gamma & \mathrm{c}\beta\,\mathrm{c}\gamma \end{pmatrix},$$

where c expresses cos,

s expresses sin,

α, β, γ—Z-Y-X Euler angles.

Then

$$\boldsymbol{u}_i = \frac{\boldsymbol{OB}_i - \boldsymbol{OP} - \boldsymbol{PP}_i}{\left|\boldsymbol{OB}_i - \boldsymbol{OP} - \boldsymbol{PP}_i\right|} = \frac{\boldsymbol{b}_i - \boldsymbol{p} - \boldsymbol{R} \bullet \boldsymbol{r}_i^{\mathrm{p}}}{\left|\boldsymbol{b}_i - \boldsymbol{p} - \boldsymbol{R} \bullet \boldsymbol{r}_i^{\mathrm{p}}\right|}.$$

3 Cable Tension Solution

From the definition of CDPM with redundant cables, one knows the number of tension distributions is infinite. The optimal tension distribution need be found with an objective function, e.g., the energy of the actuators. The optimization problem can then be described as

$$\min z = \boldsymbol{C}^{\mathrm{T}}\boldsymbol{T},\quad \text{s.t.} \begin{cases} \boldsymbol{A}\cdot\boldsymbol{T} = \boldsymbol{W}, \\ \boldsymbol{T}_{\min} \leqslant \boldsymbol{T} \leqslant \boldsymbol{T}_{\max}, \end{cases} \tag{3}$$

where $\boldsymbol{T}_{\min}$—Lower tension limit,
$\boldsymbol{T}_{\max}$—Upper tension limit,
$\boldsymbol{C} = (c_1, c_2, \cdots, c_m)^{\mathrm{T}}$.

Here, c_i is a constant. If take the sum of tensions in the cable as the objective function, one need c_i=1, for i=1, 2, $\cdots$, m. For a completely restrained CDPM, the solution set is a line segment, and the optimal tension distribution can be obtained easily and fast. For an n-DOF CDPM with n+2 cables, the kernel of structure matrix $\boldsymbol{A}$ lies in a two-dimensional space. Thus, we are able to divide the structure matrix $\boldsymbol{A}$ into two parts as

$$\begin{pmatrix}\boldsymbol{A}_1 & \boldsymbol{B}\end{pmatrix}\cdot\begin{pmatrix}\boldsymbol{T}_{\mathrm{a}} \\ \boldsymbol{T}_{\mathrm{b}}\end{pmatrix} = \boldsymbol{W}, \tag{4}$$

where $\boldsymbol{A}_1$—A n-by-n invertible matrix,
$\boldsymbol{B}$—n-by-2 matrix,
$\boldsymbol{T}_{\mathrm{a}}$—$n$-dimensional vector,
$\boldsymbol{T}_{\mathrm{b}}$—Two-dimensional vector.

$\boldsymbol{T}_{\mathrm{a}}$ can be related to $\boldsymbol{T}_{\mathrm{b}}$ by

$$\boldsymbol{T}_{\mathrm{a}} = \boldsymbol{A}_1^{-1}\boldsymbol{W} - \boldsymbol{A}_1^{-1}\boldsymbol{B}\boldsymbol{T}_{\mathrm{b}}. \tag{5}$$

Because $t_{\min} \leqslant t_i \leqslant t_{\max}$, i=1, 2, $\cdots$, m, $\boldsymbol{T}_{\mathrm{a}}$ also should satisfy this constraint. Let $\boldsymbol{T}_{\mathrm{b}} = [x, y]^{\mathrm{T}}$. Then $\boldsymbol{T}_{\min}^n \leqslant \boldsymbol{T}_{\mathrm{a}} \leqslant \boldsymbol{T}_{\max}^n$ can be rewritten as

$$\boldsymbol{T}'_{\min} \leqslant \boldsymbol{\Phi}\cdot\begin{pmatrix}x \\ y\end{pmatrix} \leqslant \boldsymbol{T}'_{\max}, \tag{6}$$

where $\boldsymbol{T}'_{\min} = \boldsymbol{T}_{\min}^n - \boldsymbol{A}_1^{-1}\boldsymbol{W}$,
$\boldsymbol{T}'_{\max} = \boldsymbol{T}_{\max}^n - \boldsymbol{A}_1^{-1}\boldsymbol{W}$,
$\boldsymbol{\Phi} = -\boldsymbol{A}_1^{-1}\boldsymbol{B}$.

Where $\boldsymbol{T}_{\min}^n$ and $\boldsymbol{T}_{\max}^n$ are the first n elements of $\boldsymbol{T}_{\min}$ and $\boldsymbol{T}_{\max}$, respectively. Then Eq. (3) can be rewritten as

$$\min z = \boldsymbol{\lambda}\begin{pmatrix}x & y\end{pmatrix}^{\mathrm{T}} + h,\quad \text{s.t.} \begin{cases} T_{\min} \leqslant x, y \leqslant T_{\max}, \\ \boldsymbol{T}'_{\min} \leqslant \boldsymbol{\Phi}\cdot\begin{pmatrix}x \\ y\end{pmatrix} \leqslant \boldsymbol{T}'_{\max}, \end{cases} \tag{7}$$

where $\boldsymbol{\lambda} = (c_{n+1} \quad c_{n+2}) - \boldsymbol{C}_n^{\mathrm{T}}\boldsymbol{A}_1^{-1}\boldsymbol{B}$,
$h = \boldsymbol{C}_n^{\mathrm{T}}\boldsymbol{A}_1^{-1}\boldsymbol{W}$,
$\boldsymbol{C}_n^{\mathrm{T}} = (c_1, c_2, \cdots, c_n)$.

For a 2-DOF CDPM with four cables, the most complex case of the solution set is only a hexagon. Thus, this optimization problem is not difficult to solve. In fact, the solution can be obtained by linear programing or by the method proposed by BORGSTROM, et al[19]. However, as the number of DOFs increases, the solution set becomes complex. To address this increased complexity, a new and efficient optimization method for the n-DOF CDPM with redundant cables is proposed in this paper.

4 Proposed Rapid Optimization Method

Eq. (7) is a linear programming problem, and it can be solved by the simplex method. Furthermore, the feasible solution set to Eq. (7) is a convex polygon as shown in Fig. 2. The geometry property of convex polygon can be used to improve the computational efficiency[23].

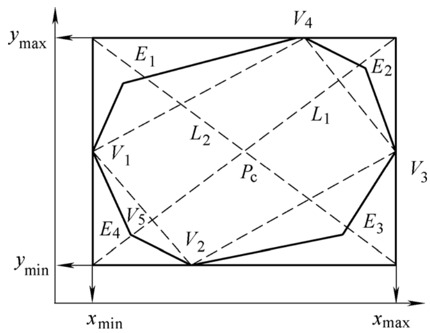

Fig. 2. Solution set of the optimization problem

4.1 Projection algorithm

In general, a solution for a linear programming problem must be an extreme point. The edges of the solution set for the optimization problem can be divided into four parts E_1 to E_4, as shown in Fig. 2. One can find an optimal point on the corresponding part of the edges with respect to symbols λ_1 and λ_2 in Eq. (7). This paper just introduction the case that λ_1 and λ_2 are positive, and the cases can be easily deduced from it. The optimal point is therefore on the edge E_4. The next problem is to obtain the two lines intersecting at the optimal point (e.g., V_1V_5 and V_2V_5) and the ranges of x and y, respectively.

Although it is easy to obtain the ranges of x and y, it is difficult to obtain the intersecting lines $L_x(V_2V_5)$ and L_y (V_1V_5). Therefore, the two lines intersecting at the optimal point(V_5) should be found. Here, finding line L_x and $y_{\min}$ are described, and the processes for determining L_y, $y_{\max}$, $x_{\max}$ and $x_{\min}$ can be deduced from this description. To improve the efficiency, the linear matrix inequality (6) is first rewritten as: $t_{li} \leqslant x + k_i y \leqslant t_{ri}$, $i = 1, 2, \cdots, n$, and l and r represent the left and right side of the inequality, respectively. Then, it is easy to compute the symbol of the slope and range of y. Let L_x^1 and L_x^2 denote the two lines intersecting at point V_2. The main steps of the projection algorithm can be described as follows:

(1) Let $y_{\min}=T_{\min}$, $L_x^1: y=T_{\min}$ and $L_x^2: y=T_{\min}$.

(2) Select two inequalities from the linear matrix inequality (6): $t_{li} \leqslant x+k_i y \leqslant t_{ri}$, $t_{lj} \leqslant x+k_j y \leqslant t_{rj}$, $i=1, 2, \cdots, n$, $j=1, 2, \cdots, n$, and $i \neq j$. Moreover, there are $q=n(n-1)/2$ combinations for the selection.

(3) If $k_i>k_j$ and $T_{\min}<(t_{li}-t_{rj})/(k_i-k_j)<T_{\max}$, then L_x^1 : $t_{li}=x+k_i y$, L_x^2: $t_{rj}=x+k_j y$, and $y_{\min}=(t_{li}-t_{rj})/(k_i-k_j)$. If $k_i<k_j$ and $T_{\min}<(t_{ri}-t_{lj})/(k_i-k_j)<T_{\max}$, then L_x^1: $t_{ri}=x+k_i y$, L_x^2 : $t_{rj}=x+k_j y$, and $y_{\min}=(t_{ri}-t_{lj})/(k_i-k_j)$. When $k_i=k_j$, the two lines are parallel, and they do not need to be calculated.

(4) If all of the combinations have been computed, one can obtain the intersecting lines and the range of y. If they are not computed, go to step (3).

The flowchart of the projection algorithm is shown in Fig. 3. After obtaining the intersecting lines, line L_x and line L_y can be defined by the slope. The process can be described as follows.

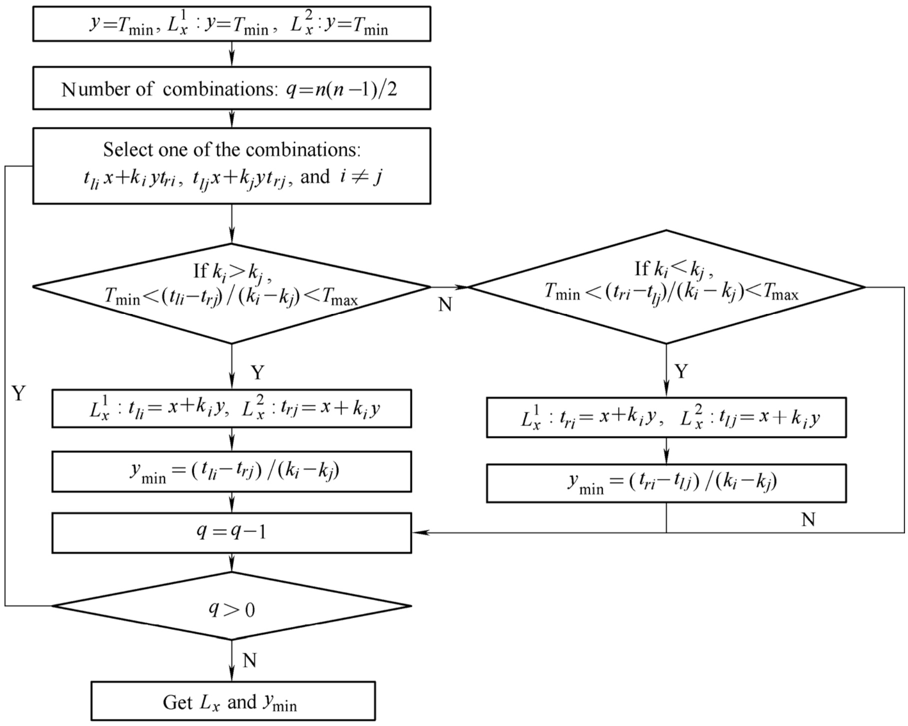

Fig. 3. Flowchart of the projection algorithm

(1) If the slopes of the intersecting lines are both negative, then line L_x is the line whose slope is larger, and the slope of line L_y is smaller.

(2) If the slopes of the intersecting lines are different, then line L_x (L_y) are the lines whose slope is negative.

(3) If the slopes of the intersecting lines are both positive by convex analysis, then the optimal point can be obtained. The optimal point is at point V ($x_{\min}$, $y_{\min}$), as shown in Fig. 4.

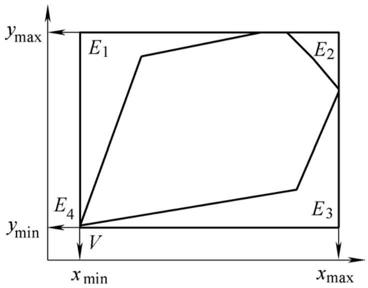

Fig. 4. Edge $E4$ is only a point

Now, the projection algorithm is obtained. For the completely restrained CDPM, the optimal point V_1 can be found by using the projection algorithm, as shown in Fig. 5. Furthermore, once one obtains the ranges of x and y, a feasible point can be found.

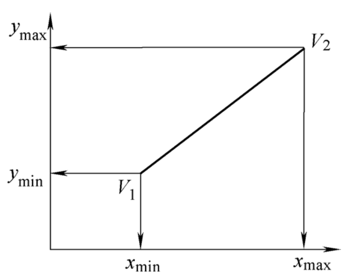

Fig. 5. Optimal point of a completely restrained CDPM

Theorem 1: Point $P_c=[(x_{\min}+x_{\max})/2, (y_{\min}+y_{\max})/2]$ is in the feasible set of Eq. (7), where $x_{\min}$ and $x_{\max}$ are the minimum and maximum value of x, and $y_{\min}$ and $y_{\max}$ are the minimum and maximum value of y.

Proof: Because the feasible set is a convex set, one can find a feasible point on every side of the rectangle, i.e., V_1

to V_4, as shown in Fig. 2. Diagonal line L_1 must be located between line V_1V_4 and line V_2V_3, and diagonal line L_2 between line V_1V_2 and line V_3V_4. Because P_c is the intersection of L_1 and L_2, P_c is within the quadrilateral $V_1V_2V_3V_4$. Therefore, point P_c is in the feasible set. Although one can only find three points sometimes, i.e., one of the three points is a vertex of the rectangle, it is easy to prove that P_c is a feasible point.

Based on **Theorem 1**, one can fast obtain a feasible solution of Eq. (7). It can be applied as the starting point of the simplex method. Furthermore, because point P_c is nearly at the middle of the feasible set, it is a candidate method for avoiding the operating point on the lower tension limit.

4.2 Algorithm for determining the optimal point

If one of the slopes of line L_x and line L_y is positive, the optimal point can be found, as shown in Fig. 4. When the slopes of line L_x and line L_y are both negative, the solution set of the optimization problem (7) can be classified into six cases, as shown in Fig. 6.

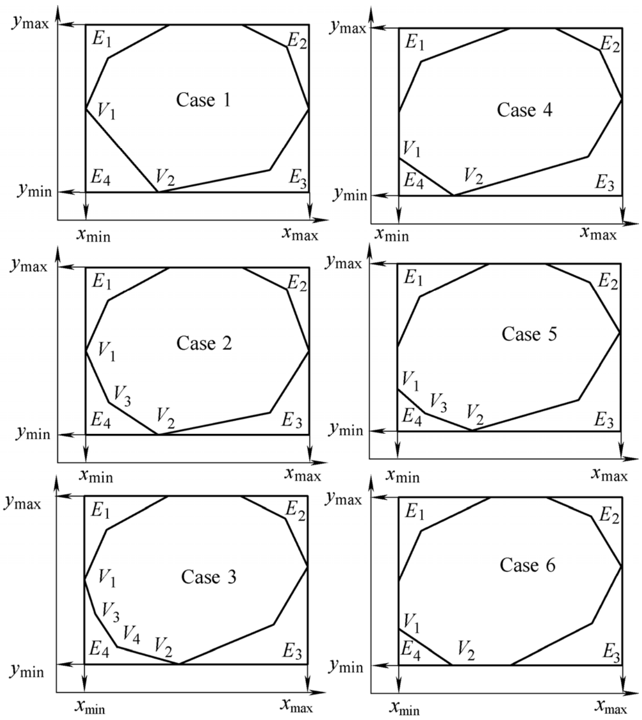

Fig. 6. Six cases of the solution set

The algorithm for determining the optimal point in each case is described as follows.

Case 1: Line L_x and line L_y are the same line, and $x_{min} \neq T_{min}$ and $y_{min} \neq T_{min}$. In this case, the optimal point is V_1 or V_2. If $-\lambda_1/\lambda_2$ is larger than the slope of line V_1V_2, then V_2 is the optimal point. Otherwise, V_1 is the optimal point.

Case 2: Line L_x and line L_y are different, and $x_{min} \neq T_{min}$ and $y_{min} \neq T_{min}$, and V_3 is a feasible point. In this case, the optimal point must be one of the three vertexes(V_1, V_2 and V_3). If $-\lambda_1/\lambda_2$ is larger than the slope of V_2V_3, then V_2 is the optimal point. If $-\lambda_1/\lambda_2$ is smaller than the slope of V_1V_3, then V_1 is the optimal point. Otherwise, V_3 is the optimal point.

Case 3: Line L_x and line L_y are different, and $x_{min} \neq T_{min}$ and $y_{min} \neq T_{min}$, and the intersection point of line L_x and line L_y is not a feasible point. In this case, it is not easy to determine the optimal point. One can apply V_1 or V_2 to initialize the simplex method. Thus, the optimal point can be found fast. On the other hand, based on convex analysis, one knows that the slope of the line intersecting at the optimal point is larger than the slope of L_y and smaller than the slope of L_x. Furthermore, its corresponding inequality can be described as: $x+ky \geqslant t_l$, where $k>0$ and $t_l>0$. Thus, the number of the lines satisfying the two conditions is small. Moreover, the slopes from line L_x to line L_y are descending. For instance, the slope of line V_1V_3 is smaller than that of line V_3V_4, and the slope of line V_3V_4 is smaller than that of line V_4V_2. Thus, the number of intersection points is small as well. The optimal point can also be determined by checking whether the intersection point is feasible and is the smallest.

Case 4: Line L_x and line L_y are the same, and $x_{min}=T_{min}$ or $y_{min}=T_{min}$. In this case, V_2 (V_1) can be obtained by the projection algorithm first, and then $V_1(V_2)$ can be determined because line L_x and line L_y are the same. The optimal point is V_1 or V_2. If $-\lambda_1/\lambda_2$ is larger than the slope of line V_1V_2, then V_2 is the optimal point. Otherwise, V_1 is the optimal point.

Case 5: Line L_x and line L_y are different, and $x_{min}=T_{min}$ or $y_{min}=T_{min}$. In this case, one should find $V_1(V_2)$ first, and it can be used as the start point of the simplex method as well. Further, the vertex V_1 is the smallest of the feasible intersection points between line $x=T_{min}$ ($y=T_{min}$) and the lines whose slopes are smaller than L_y (bigger than L_x), and the corresponding inequality can be written as $x+ky \geqslant t_l$. After obtaining V_1, one can also find the optimal point by using the method in Case 3.

Case 6: Line L_x and line L_y are different, and $x_{min}=T_{min}$ and $y_{min}=T_{min}$. In this case, vertex V_1 and vertex V_2 are not known. If the two vertices are determined, then the optimal point can be found by the methods of Cases 1 through 3. Moreover, the method for determining V_1 and V_2 is the same as Case 5.

The flowchart of the new optimization method, when λ_1 and λ_2 are positive, is shown in Fig. 7.

5 Simulation Experiments

To verify the proposed optimization method for tension distribution, simulation experiments were conducted on a 6-DOF CDPM with eight cables, as shown in Fig. 8, where the winches is installed on the vertices of the fixed platform. The fixed platform is a cube, and each side has a width of 1 m. The moving platform is a 0.3 m×0.2 m×0.1 m block, and the center of mass is at the geometric center of the block. The range of each cable tension is 1 to 540 N. The Euler angles α, β, and γ of the CDPM are 2°, 3° and 1°, respectively.

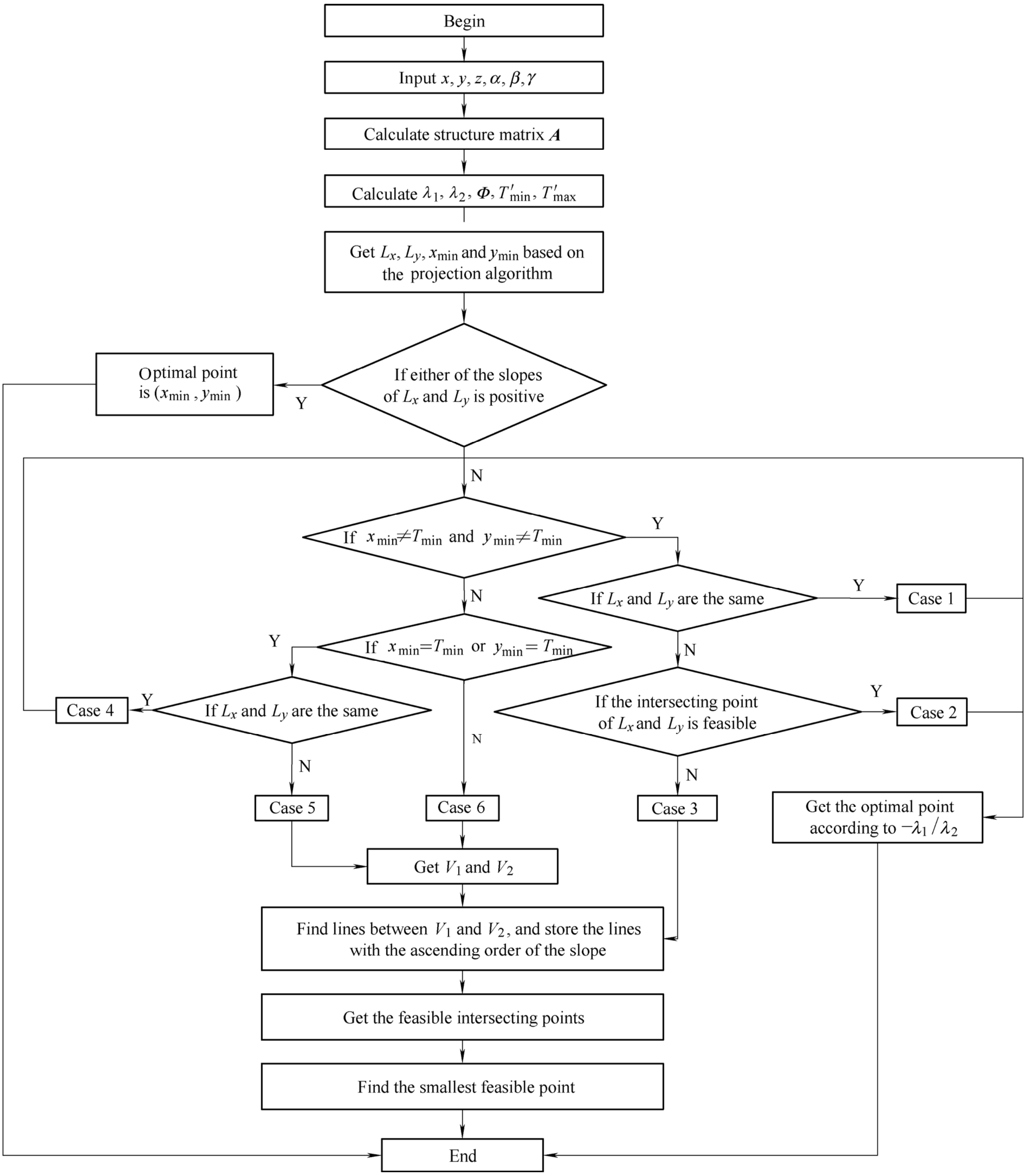

Fig. 7. Flowchart of the optimization method when λ_1 and λ_2 are positive

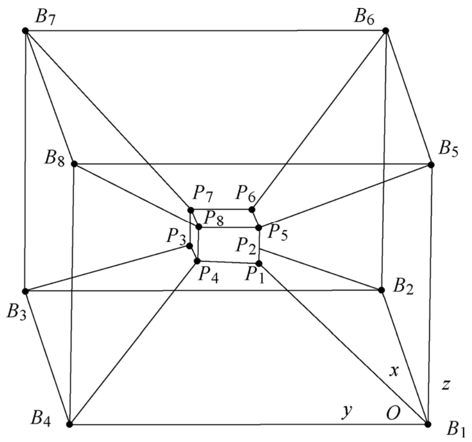

Fig. 8. Structural diagram of the 6-DOF CDPM with eight cables

The optimization process ware was implemented in Matlab on an Intel Core i3-2120 3.3 GHz with 4G RAM. The computational efficiency of the new optimization method were compared with the simplex method. Here, the sum of the tensions was taken as the performance index. First, we fixed the external wrench and changed the position of the moving platform. The range of x, y, and z were 0.4 to 0.6 m, and the sample interval is 0.01 m. The simulation results are shown in Table 1. We then fixed the coordinate of the moving platform and varied the external wrench in the range of 4.5 to 6.5 N, with a step size of 0.5 N. The range of the external moment was 0.4 to 0.8 N • m at a 0.1 N increment. The simulation results are given in Table 2.

Table 1. Total computational time of the proposed method and simplex method when the external wrench is fixed

External wrench	Proposed method t_p/s	Simplex method t_s/s
[5.0, 5.5, 5.0, 0.5, 0.4, 0.5]	6.03	35.55
[5.5, 5.0, 5.5, 0.4, 0.5, 0.4]	5.88	34.23
[5.5, 5.0, 5.5, 0.4, 0.5, 0.4]	5.85	34.33

Table 2. Total computational time of the proposed method and simplex method as the coordinate is fixed

Coordinate of the moving platform/m	Proposed method t_p/s	Simplex method t_s/s
[0.5, 0.5, 0.5]	4.57	54.63
[0.5, 0.55, 0.5]	2.82	50.73
[0.45,0.5, 0.45]	4.43	50.30

From the simulation results in Tables I and II, one can see that total computing time of proposed method t_p was one order of magnitude less than that of simplex method (t_s), and thus, it can satisfy the real-time computational requirement. Now, let the external wrench $\boldsymbol{W}$=[5.5, 5, 5.5, 0.4, 0.5, 0.4]^T (force in N and moment in N. m), and let the moving platform move on the line $x=y=z$. For the linear trajectory, the start point was [0.4, 0.4, 0.4](m), the end point was [0.65, 0.65, 0.65](m) and the sample interval was 0.002 m. First, one can obtain a feasible solution for Eq. (7) based on **Theorem 1**, and the tension distribution is shown in Fig. 9. One can see that this method avoids the lower tension limit successfully, but the tensions are too large.

Moreover, the tension distribution by using the proposed method is shown in Fig. 10. One can see that the tensions are considerably smaller than tensions obtained by **Theorem 1**, and it is continuous as well. On the other hand, one can define $\|\mathbf{T}\|_2$ as the objective function, i.e., quadratic programming, and use an active-set algorithm to obtain the optimal tension distribution. One can find that the tension distributions are the same as those obtained by using linear programming. It is known that the optimal tension distribution with linear programming can be discontinuous in theory, and the quadratic programming can obtain continuous tension distribution. Thus, the discontinuous tension distribution does not happen often.

Further, one can fix the moving platform at point [0.5, 0.5, 0.5] (m) and change the external wrench $\boldsymbol{W}=[w_1, w_2, \cdots, w_6]^T$ according to: w_1=5(N), $w_4=w_5=w_6$=0.4 (N • m), and $w_2=w_3=6\sin\varphi$ (N), where $\varphi\in$[45°, 90°] with a step size of 0.5°. The tension distribution is shown in Fig. 11. One can see that the tension distribution is continuous. One can also know that the tension distribution obtained by using quadratic programming is the same with the linear programming. However, tensions such as t_1 and t_4 are considerably smaller compared with those in other cables, and tension t_1 is nearly constant and on the lower tension limit. The distribution of tensions calculated by applied **Theorem 1**(shown in Fig. 9**)** can be applied to solve this problem, but these tensions are larger. Thus, the proposed method need be developed to the distribution more uniform.

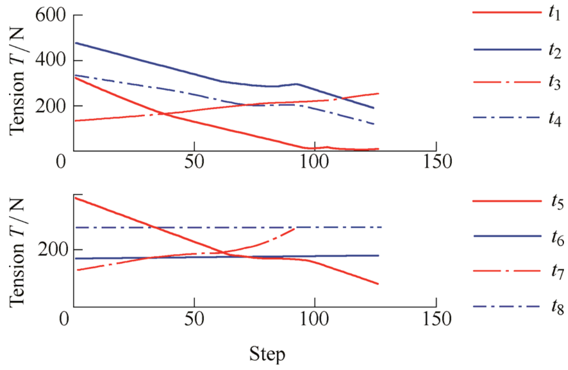

Fig. 9. Tension distribution obtained by Theorem 1

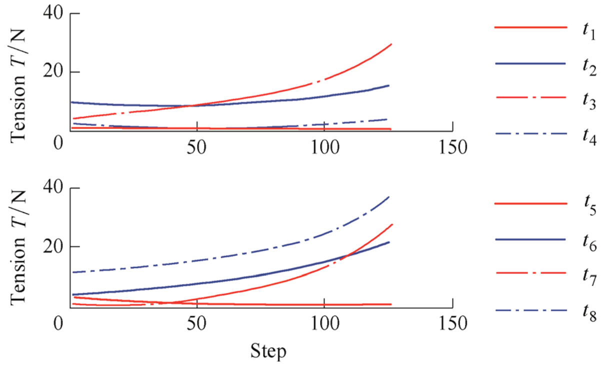

Fig. 10. Tension distribution of the CDPM when the position is varied and the external wrench is constant

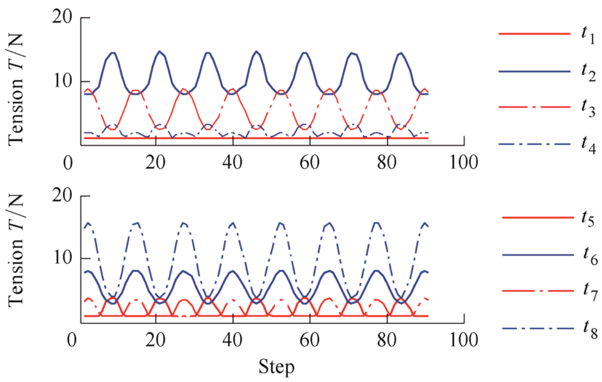

Fig. 11. The tension distribution of the CDPM when the external wrench is changed and the position is fixed

6 Conclusions

(1) A new and rapid method is proposed for optimizing the tension distribution of CDPM with redundant cables.

(2) The computational efficiency of the new optimization method is considerably higher than the simplex method, and it can be executed in real time.

(3) The simulation results are also verified the method for avoiding the operating point on the lower tension limit.

(4) The tension distribution is continuous in all of the simulation experiments although the tension distribution may be discontinuous in theory.

References

[1] YUASA K, MAE Y, INOUE K, et al. A hybrid drive parallel arm for heavy material handling[J]. *IEEE Transactions on Robotics and Automation*, 2002, 9(1): 45–54.

[2] BEHZADIPOUR S, KHAJEPOUR A. Design of reduced DOF parallel cable-based robots[J]. *Mechanism and Machine Theory*, 2004, 39(10): 1051–1065.

[3] HILLER M, FANG S, MIELCZAREK S, et al. Design, analysis and realization of tendon-based parallel manipulators[J]. *Mechanism and Machine Theory*, 2005, 40(3): 429–445.

[4] LAFOURCADE P, LLIBER M, REBOULE C. Design of a parallel wire-driven manipulator for wind tunnels[C]//*Proceedings of the Workshop on Fundamental Issues and Future Directions for Parallel Mechanisms and Manipulators*, Quebec City, Quebec, Canada, October 3–4, 2002: 187–194.

[5] WANG W L, DUAN B Y. A new type of flexible parallel link manipulator actuated by cable[J]. *Control Theory and Application*, 2001, 18(3): 328–332.

[6] MAO Y, JIN X, DUTTA G G, et al. Human movement training with a cable driven arm exoskeleton(CAREX)[J]. *IEEE Transactions on Systems and Rehabilitation Engineering*, 2015, 23(1): 84–92.

[7] LAU D, EDEN J, OETOMO D, et al. Musculoskeletal static workspace analysis of the human shoulder as a cable-driven robot[J]. *IEEE/ASME Transactions on Mechatronics*, 2015, 20(2): 978–984.

[8] MUSTAFA S K, YANG G L, YEO S H, et al. Self-calibration of a biologically inspired 7 DOF cable-driven robotic arm[J]. *IEEE/ASME Transactions on Mechatronics*, 2008, 13(1): 66–75.

[9] YUAN H, COURTEILLE E, DEBLAISE D. Static and dynamic stiffness analyses of cable-driven parallel robots with non-negligible cable mass and elasticity[J]. *Mechanism and Machine Theory*, 2015, 85: 54–81.

[10] LAU D, OETOMO D, HALGAMUGE S K. Inverse dynamics of multilink cable-driven manipulators with the consideration of joint interaction forces and moments[J]. *IEEE Transactions on Robotics*, 2015, 31(2): 479–488.

[11] PHAM C B, YEO S H, YANG G L, et al. Force-closure workspace analysis of cable-driven parallel mechanisms[J]. *Mechanism and Machine Theory*, 2006, 41(1): 53–69.

[12] OUYANG B, SHANG W W. Efficient computation method of force-closure workspace for 6-DOF cable-driven parallel manipulators[J]. *Journal of Mechanical Engineering*, 2013, 49(15): 34–41.

[13] OUYANG B, SHANG W W. A new computation method for the force-closure workspace of cable-driven parallel manipulators[J]. *Robotica*, 2015, 33(3): 537–547.

[14] GOUTTEFARDE M, DANEY D, MERLET J P. Wrench-feasible workspace of parallel cable-driven mechanisms[C]//*IEEE International Conference on Robotics and Automation*, Roma, Italy, April 10–14, 2007: 1492–1497.

[15] BOSSCHER P, RIECHEl A T, EBERT-UPHOFF I. Wrench-feasible workspace generation for cable-driven robots[J]. *IEEE Transactions on Robotics*, 2006, 22(5): 890–902.

[16] OUYANG B, SHANG W W. Wrench-feasible workspace based optimization of fixed and moving platforms for cable-driven parallel manipulators[J]. *Robotics and Computer-Integrated Manufacturing*, 2014, 30(6): 629–635.

[17] FANG S Q, FRANITZA D, TORLO M, et al. Motion control of a tendon-based parallel manipulator using optimal tension distribution[J]. *IEEE/ASME Transactions on Mechatronics*, 2004, 9(3): 561–568.

[18] LI H, ZHANG X Y, YAO R, et al. Optimal force distribution based on slack rope model in the incompletely constrained cable-driven parallel mechanism of FAST telescope[J]. *Cable-Driven Parallel Robots Mechanisms and Machine Science*, 2013, 12: 87–102.

[19] BORGSTROM P H, JORDAN B L, BORGSTROM B J, et al. NIMS-PL: A cable-driven robot with self-calibration capabilities[J]. *IEEE Transactions on Robotics*, 2009, 25(5): 1005–1015.

[20] MIKELSONS L, BRUCKMANN T, HILLER M, et al. A real-time capable force calculation algorithm for redundant tendon-based parallel manipulators[C]//*IEEE International Conference on Robotics and Automation*, Pasadena, CA, May 19–23, 2008: 3869–3874.

[21] BORGSTROM P H, JORDAN B L, SUKHATME G S, et al. Rapid computation of optimally safe tension distributions for parallel cable-driven robots[J]. *IEEE Transactions on Robotics*, 2009, 25(6): 1271–1281.

[22] HASSAN M, KHAJEPOUR A. Analysis of bounded cable tensions in cable-actuated parallel manipulators[J]. *IEEE Transactions on Robotics*, 2011, 27(5): 891–900.

[23] BOYD S, VANDENBERGHE L. *Convex optimization*[M]. Cambridge: United Kingdom at the University Press, 2009.

Biographical notes

OUYANG Bo, born in 1989, is currently a master candidate at *Department of Automation, University of Science and Technology of China*. He received his bachelor degree from *Southwest University, China*, in 2011. His research interests include parallel robot and optimization.
E-mail: boouyang2-c@my.cityu.edu.hk

SHANG Weiwei, born in 1981, is currently an associate professor at *Department of Automation, University of Science and Technology of China*. He received his PhD degree from *University of Science and Technology of China*, in 2008. His research interests include parallel robots, humanoid robots and robot vision.
Tel: +86-551-63601332; E-mail: wwshang@ustc.edu.cn